

# Poly(methacrylic acid) Grafts Grown from Designer Surfaces: The Effect of Initiator Coverage on Polymerization Kinetics, Morphology, and Properties

Edmondo M. Benetti,<sup>†</sup> Erik Reimhult,<sup>‡</sup> Johannes de Bruin,<sup>†</sup> Szczepan Zapotoczny,<sup>§</sup> Marcus Textor,<sup>‡</sup> and G. Julius Vancso<sup>\*,†</sup>

*Materials Science and Technology of Polymers, MESA<sup>+</sup> Institute for Nanotechnology, University of Twente, P.O. Box 217, NL-7500 AE Enschede, The Netherlands, Laboratory for Surface Science and Technology, Department of Materials, ETH Zurich, Wolfgang-Pauli-Strasse 10, CH-8093 Zurich, Switzerland, and Faculty of Chemistry, Jagiellonian University, Ingardena 3, PL-30-060 Cracow, Poland*

*Received July 1, 2008; Revised Manuscript Received November 12, 2008*

**ABSTRACT:** Poly(methacrylic acid) (PMAA) films were photografted by iniferter-mediated polymerization from self-assembled monolayers (SAMs) of initiator molecules immobilized on Au via disulfide linkages and mixed with disulfide alkanes. The influence of initiator coverage on the growth rates of film thickness, surface morphology, and nanoscale mechanics was studied. Film thickness was measured by ellipsometry and atomic force microscopy (AFM), whereas mechanical performance was assessed by AFM compression force. Remarkably, the film thickness growth rate by ellipsometry did not show any significant variation with initiator coverage. However, surface morphology visualized by AFM showed clear influences of the composition of the initiating SAMs, which directly affected the rate of termination reactions. To investigate the early stages in the grafting process, polymerization was performed in situ using a quartz crystal microbalance with dissipation monitoring setup (QCM-D). The mass increment during the photografting was evaluated using concentrated and diluted SAMs of the initiator. A remarkably higher number of grafted chains in the case of concentrated SAMs was observed. By comparing this result with the AFM measurements on the obtained films, we recognized a broader chain length distribution, consequent to termination reactions in dense systems, to influence the surface morphology of the layers.

## Introduction

In the past decade, surface-initiated polymerization (SIP) methods have been proven to be solid fabrication techniques for the surface modification of metals, semiconductors, and polymeric supports using grafted macromolecules. The technological advances that accompanied the development of SIP allowed not only the fabrication of simple polymeric coatings but also the synthesis of responsive nanosystems,<sup>1–3</sup> composite interfaces,<sup>4–6</sup> and smart biological platforms.<sup>7–12</sup> Following the fundamental works of R  he and Prucker,<sup>13,14</sup> who systematically studied the surface-confined synthesis of polymers from flat surfaces, the development of different SIP techniques has closely followed the advances in controlled polymerization methods, especially those based on radical mechanism. Atom transfer radical polymerization (ATRP),<sup>15–17</sup> reversible addition fragmentation–chain transfer processes (RAFT),<sup>18,19</sup> and nitroxide-mediated radical polymerization<sup>20,21</sup> were mostly employed in the grafting of polymeric films, which are often called polymer brush layers in cases in which the density of immobilized macromolecules is high enough to induce the stretching out of the chains from the solid support.

In all of the mentioned methodologies, the universal platform for the grafting process included SAMs of initiators. SAMs can be easily prepared on a variety of metallic and nonmetallic substrates. In addition, their composition can theoretically be easily tuned by mixing adsorbates bearing initiator functionalities with corresponding inert molecules characterized by similar anchoring chemistry.<sup>22–25</sup> Platform engineering of the precursor SAMs by using mixed monolayers (or alternatively, ac-

complishing surface dilution of initiator species) was used to investigate the effects of the grafting site density on the morphology of the grown polymer chains.<sup>26</sup>

Numerous studies reported that the thickening rate of grafted films decreased with increasing dilution of the initiator at the precursor surface.<sup>26–30</sup> Possible kinetic or morphological effects caused by radical recombination in the case of the very high surface concentration of growing chains was not univocally recognized, with the exception of an irreversible deceleration of the film's growth rate, but specifically followed long reaction periods.<sup>31,32</sup> The latter phenomenon was reported to limit the maximum achievable film thickness to some hundreds of nanometers in the case of ATRP-based systems after several hours of reaction.<sup>31</sup>

Thus, although it has not been systematically addressed yet, the composition of the initiating surface may have direct consequences on the thickness, the density, and the morphology of the layers. In addition, varying the surface density of initiators could influence the polymerization mechanism itself, which would also affect the chain length distribution of the grafted polymer. The degree of polydispersity characteristics of a grafted system is difficult to estimate: direct measurements on detached films are often a difficult task, and the estimation by using samples synthesized from sacrificial initiator in solution may not always be representative of the reality of the surface grafting process. Thus, other parameters such as the thickening rate, the surface nano/micromorphology, and swelling properties may be used for interpreting the factors that influence the grafting mechanism.

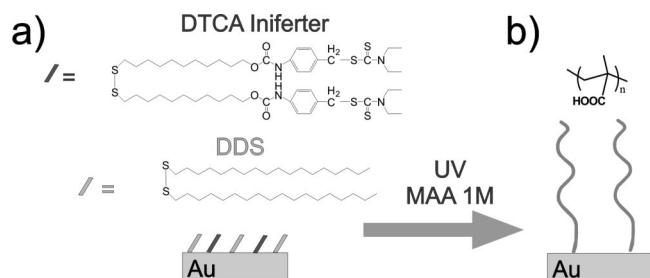
Aiming to investigate how the composition of initiating SAMs could influence the grafting of polymer films, we report here a systematic study focused on the role of initiator surface coverage on the kinetics, the morphology, and the properties of photopolymerized poly(methacrylic acid) (PMAA) layers.

\* Corresponding author. E-mail: g.j.vancso@utwente.nl.

<sup>†</sup> University of Twente.

<sup>‡</sup> ETH Zurich.

<sup>§</sup> Jagiellonian University.

Scheme 1. Synthesis of PMAA Grafts from Mixed SAMs on Au<sup>a,b</sup>

<sup>a</sup> (a) Formation of mixed initiating SAMs of DTCA initiator and DDS diluent agent.

<sup>b</sup> (b) Photopolymerization of methacrylic acid and formation of surface-tethered PMAA films.

The initiating system was based on dithiocarbamate-bearing adsorbates that, in the form of disulfides (Scheme 1), can easily self-assemble on the Au surface. We have recently shown that robust UV-SIP could be successfully performed from SAMs of such initiators on gold surfaces.<sup>33</sup> The dithiocarbamate species, introduced as photoinitiators (or iniferters: initiator–transfer–terminator agents) by Otsu,<sup>34,35</sup> have the peculiarity of cleaving upon UV irradiation, forming a radical pair constituted by a reactive carbon radical that initiates the polymerization and a less reactive, sulfur-centered radical that can act as a reversible capping agent during the polymerization process. Disulfide-based initiators were thus used in the presence of similar but inert disulfide species to form mixed monolayers of variable relative composition. (See the Experimental Section.) PMAA was subsequently photografted from SAMs with different surface concentration of the initiator, and the thickening rate of the films was evaluated by *ex situ* ellipsometry. The surface morphology and the swelling properties of different films grafted from full and diluted monolayers of initiators were investigated by atomic force microscopy (AFM), which showed the relevant influence of the composition of the SAM on the characteristics of the subsequently grafted polymer films.

To get more insight into the mechanism of polymerization and the influence of the surface concentration of initiating species, we measured the actual increment in hydrated polymer mass in real time in the early stages of the process by quartz crystal microbalance with dissipation monitoring (QCM-D).

The combination of different characterization techniques showed a relevant influence by the surface density of initiating species on the morphology and the properties of the subsequently grafted polymer films.

## Experimental Section

**Materials.** Methacrylic acid (MAA) and methyl methacrylate (MMA) were obtained from Sigma and were purified from inhibitors by condensation under high vacuum. The disulfide photoinitiator dithiodiundecane-11,11-diylbis[4(((diethylamino)carbonothioyl)thioethyl)phenyl]carbamate (DTCA) was synthesized as previously reported.<sup>33</sup> 1,2-dioctadecyldisulfane (DDS) was obtained by oxidation of octadecane-1-thiol (ODT, Sigma) in chloroform using an equimolar aqueous solution of iodine and potassium iodide (Merck and Sigma, respectively). Gold substrates were purchased from Ssens B.V. (Hengelo, The Netherlands). All solvents were used in high purity, and milli-q water was obtained from a Millipore system (Millipore S.A.S., Molsheim, France).

**Photopolymerization.** In a typical procedure, 1 mM mixed chloroform solutions of DTCA and DDS with molar ratios of initiator equal to 0.2, 0.4, 0.6, 0.8, and 1.0 were used to form the initial SAMs. Gold substrates with an area of 6 cm<sup>2</sup> were cleaned with a piranha (30/70% H<sub>2</sub>O<sub>2</sub>/H<sub>2</sub>SO<sub>4</sub>) solution, and after extensive

rinsing with milli-q water, ethanol and dichloromethane were immersed in the corresponding DTCA/DDS solution overnight at room temperature.

The so-prepared samples were subsequently placed in a quartz flask containing a 1.0 M aqueous solution of MAA. They were extensively purged with argon and finally irradiated through a 280 nm cutoff filter for the necessary polymerization time by an array of six UV-B lamps (15W, G15T8E, Ushio, Japan, sample-to-lamp distance: 20 cm). After the photopolymerization was carried out for the desired time, the substrates were rinsed with milli-q water overnight. We grafted MMA by following similar experimental procedures with the exception of using toluene as the solvent and the final monomer concentration of 4.5 M.

**Characterization.** Contact angle measurements were performed on the SAM-functionalized gold substrates to monitor the changes in wettability following chemisorption of different relative concentrations of DTCA with respect to DDS. Static water contact angle measurements were performed by the sessile drop technique using an optical contact angle device equipped with an electronic syringe unit (OCA15, Dataphysics, Germany). This setup was then connected to a charge-coupled device (CCD) video camera. The sessile drop was deposited onto the polished surface of the materials with the syringe, and the drop contour was fit by the Young–Laplace method. Twenty measurements of each specimen were performed.

X-ray photoelectron spectroscopy (XPS) was used to evaluate the actual surface concentration of the initiator in SAMs prepared from feeding solutions containing different molar fraction of DTCA/DDS. XPS spectra were obtained on a Quantera XPS instrument (Physical Electronics) using monochromatized Al K $\alpha$  radiation (1486.6 eV) with an X-ray beam diameter of 100  $\mu$ m and an angle of 45° relative to the substrate's surface. Each sample was measured over a set of eight different locations.

To evaluate the relative concentration of DTCA on the surface, high-resolution XPS elemental scans for the O1s, N1s and C1s signals were recorded. The ratios between elemental concentrations C/N and C/O were evaluated as a function of the molar fraction of DTCA initially present in the corresponding feeding solutions ( $\Phi_{\text{DTCA}}^{\text{solution}}$ ). Thus, by combining the values obtained for each sample, we calculated the relative composition of the SAMs (expressed as  $\Phi_{\text{DTCA}}^{\text{surface}}$ ) with respect to  $\Phi_{\text{DTCA}}^{\text{solution}}$ .

The dry thickness of the subsequently grafted PMAA films was measured using a computer-controlled null ellipsometer (Philips Plasmon) working with a He–Ne laser ( $\lambda = 632.8$  nm) at an angle of incidence of 70°. The measurements were formed at 22 °C under 30% relative humidity, and the data obtained were averaged over 40 points at the surface of each sample. For the grafted PMAA layers, a refractive index of 1.475 was used.<sup>36</sup>

The surface morphology of the films was evaluated by atomic force microscopy in tapping mode (TM-AFM) using a Dimension 3100 setup (Digital Instruments, Veeco, Santa Barbara, CA) and recording topography images over several areas of each substrate. The same instrument equipped with a liquid cell was used in contact mode to evaluate the properties of the PMAA layers when immersed in PBS buffer at pH 7. To monitor the swelling behavior and the resistance to compression of the grafted PMAA, we mechanically removed (scratched) the polymer layers with plastic tweezers, and the height between the unscratched and scratched regions was measured in contact mode upon the application of variable loads by the AFM tip.

QCM-D measurements<sup>37</sup> were performed to monitor the polymer growth in the first stages of the polymerization process. AT-cut quartz crystals (Q-Sense, Gothenburg, Sweden) with a fundamental resonance frequency of 5 MHz were used as substrates for the grafting of PMAA. The gold electrode on the quartz crystal sensor was functionalized *ex situ* with initiating SAMs by following the same procedures reported in the Materials section with 0.2 and 1.0 molar ratios of DTCA to DDS, respectively. The sensors were subsequently placed inside a QCM-D chamber equipped with a liquid flow system on a Q-Sense E4 measurement system (Q-Sense, Gothenburg, Sweden). A quartz window in the chamber allowed for effective UV illumination of the sensor surface with the unit

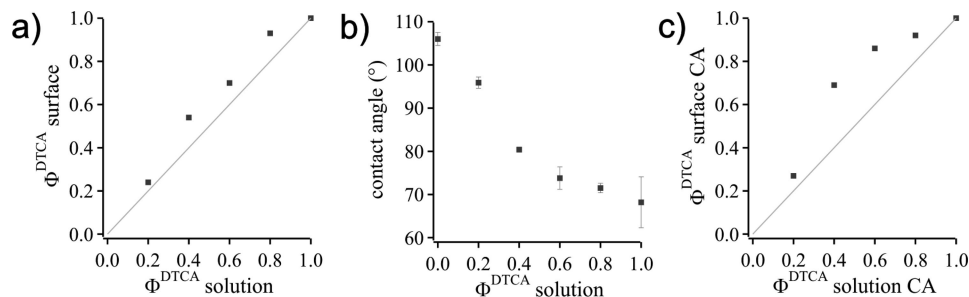


**Figure 1.** (a) Molar fraction of DTCA molecules on the SAMs ( $\Phi_{\text{DTCA}}^{\text{surface}}$ ) measured by XPS analysis and expressed as a function of the molar fraction of DTCA present in the feeding solution ( $\Phi_{\text{DTCA}}^{\text{solution}}$ ). (b) Static water contact angle values recorded on SAMs prepared from feeding solutions with different molar fraction of DTCA ( $\Phi_{\text{DTCA}}^{\text{solution}}$ ). (c) Molar fraction of DTCA molecules on the SAMs ( $\Phi_{\text{DTCA}}^{\text{surface CA}}$ ) calculated from contact angle data by using the Cassie equation and expressed as a function of the molar fraction of DTCA present in the feeding solution ( $\Phi_{\text{DTCA}}^{\text{solution CA}}$ ).

placed under an array of six UV-B lamps. Degassed MAA solution was pumped inside the system via an external syringe and was finally irradiated by the already described UV setup. The Q-Sense E4 system allows for the simultaneous recording of changes in resonant frequency ( $\Delta f$ ) and energy dissipation ( $\Delta D$ ) recorded at multiple overtones (5, 15, ..., 65 MHz). As a first approximation, the system had a mass sensitivity of 17.7 ng/cm<sup>2</sup> per Hz at 5 MHz using the Sauerbrey relation.<sup>38</sup> However, acoustic sensors such as QCM-D measure the adsorbed mass including dynamically coupled water and are sensitive to the viscoelastic properties of the adsorbed film as well.<sup>39,40</sup> Thus, to calculate the variation in grafted polymer mass, a Voigt-based model was used to fit the experimental data for  $\Delta f$  and  $\Delta D$  at several overtones, which takes the effect of viscoelasticity into account.<sup>41,42</sup> The hydrated polymer grafts were considered to be a homogeneous viscoelastic film characterized by the viscosity ( $\eta_p$ ) varying between 0.001 and 0.01 kg/ms and a swollen thickness ( $d$ ) varying between 0 and 1  $\mu\text{m}$ .

## Results and Discussion

### Formation of Mixed Initiator Self-Assembled Monolayers.

In Scheme 1, the molecular structure of the two different adsorbates, DTCA and DDS, that were used to form the mixed initiating SAMs on Au are depicted. As already described, mixed SAMs deposited from feeding solutions containing different molar ratios of the two components were prepared to investigate the role of the surface concentration of photolabile groups in the subsequent grafting of PMAA. In Figure 1, the surface composition of the SAMs, which was measured with XPS after overnight incubation, was plotted, expressing the molar fraction of DTCA in the monolayers ( $\Phi_{\text{DTCA}}^{\text{surface}}$ ) as function of the molar fraction in the feed solution ( $\Phi_{\text{DTCA}}^{\text{solution}}$ ).

As one can see from Figure 1a, the data points lie in the proximity of the line of unity slope (corresponding to no preferential adsorption of one component with respect to the other). Thus, the surface concentration of DTCA molecules can be precisely tuned by varying the  $\Phi_{\text{DTCA}}^{\text{solution}}$  of the corresponding feed solutions.

In the case of mixed precursor SAMs for SIP, several studies in the literature reported on the fine control of the actual surface concentration of initiating adsorbates as a difficult task because the thiol-based initiator molecules preferentially adsorbed in comparison to the diluent unreactive thiol.<sup>30,32</sup> In the present case, the values of  $\Phi_{\text{DTCA}}^{\text{surface}}$  compared with those of  $\Phi_{\text{DTCA}}^{\text{solution}}$  were only slightly higher (between the 15 and 35%). This effect was probably due to the higher polarity of DTCA functionalities with respect to the CH<sub>3</sub>-terminating DDS, which thus makes the chemisorption of the former compound on the Au surface energetically favored.<sup>22</sup>

The increase in the surface concentration of the more polar DTCA molecules also influenced the wettability of the initiating SAMs. As can be seen in Figure 1b, the static water contact angle measured on SAMs with different surface compositions

of the two components steadily decreased with the increase in  $\Phi_{\text{DTCA}}^{\text{solution}}$ , confirming the presence of DTCA species on the surface.

By using the obtained values of contact angles in the well-known Cassie equation, it was possible to calculate the experimental surface composition of the SAMs,<sup>43</sup> expressed as  $\Phi_{\text{DTCA}}^{\text{surface CA}}$ , as a function of the relative composition of the feeding solutions,  $\Phi_{\text{DTCA}}^{\text{solution CA}}$ . By plotting the two series of values (Figure 1c), we obtained a curve that was very similar to that obtained through the XPS analysis. Also, in this case, the experimental values lie in the vicinity but above the line of no preferential adsorption, which reflects a control over the surface composition of the SAMs and a slight energetically favored adsorption of DTCA molecules compared with DDS.

**Photografting of Poly(methacrylic acid).** The kinetics of SIP using iniferter initiators on flat surfaces was first investigated by Hadziioannou et al.<sup>44</sup> and recently by Metters et al.<sup>45</sup> In the first study, a linear increase in the film thickness with the polymerization time for the grafting of poly(methyl methacrylate) (PMMA) was found, and thus the living character of this particular SIP method was demonstrated. In the latter report, the grafting of PMMA from initiator-modified silicon oxide surfaces was investigated, and an irreversible slowing down of the polymerization with time was observed. This phenomenon translated into a nonlinear growth of PMMA layers with the irradiation time. This was described as a direct consequence of the loss of surface-tethered radicals by recombination reactions.

The number of tethered chains is directly related to the number of the initiator molecules on the surface that effectively initiate and propagate the growth of polymers. Therefore, the surface concentration, or alternatively, the distance between grafting points, is a parameter that should play a fundamental role in the subsequent film growth.

In the present study we have photopolymerized PMAA from SAMs on Au bearing different initiator concentrations deposited from solutions of 1.0, 0.8, 0.6, 0.4, and 0.2  $\Phi_{\text{DTCA}}^{\text{solution}}$  corresponding to  $\Phi_{\text{DTCA}}^{\text{surface}}$  values of 1.0, 0.9, 0.7, 0.5, and 0.2, respectively. The polymerization reactions were all performed by keeping the monomer concentration constant, and for each sample, the dry ellipsometric thickness of the synthesized PMAA layers was measured after time intervals ranging from 10 to 80 min.<sup>46</sup>

In Figures 2a–c, the dry thickness measured as a function of the polymerization time was plotted for all of the samples studied. To simplify the graphical representation, the growth rate was plotted in Figure 2a for films grafted from 1.0 SAMs (full initiator coverage), in Figure 2b for semidiluted SAMs (corresponding to 0.8, and 0.6  $\Phi_{\text{DTCA}}^{\text{solution}}$ ), and in Figure 3c for highly diluted 0.4 and 0.2 SAMs.

In general, it is interesting that very thick films up to 400 nm can be synthesized during 80 min of irradiation for the entire range of DTCA molar ratio considered. The polymerization rates



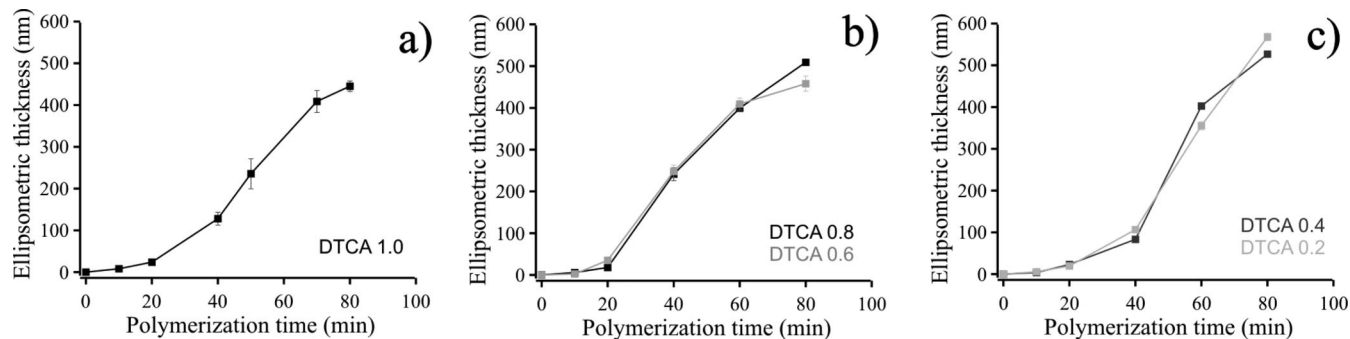


**Figure 2.** Ellipsometric thickness of PMAA films as a function of UV irradiation time plotted for films grafted from (a) 1.0, (b) 0.8 and 0.6, and (c) 0.4 and 0.2 SAMs.

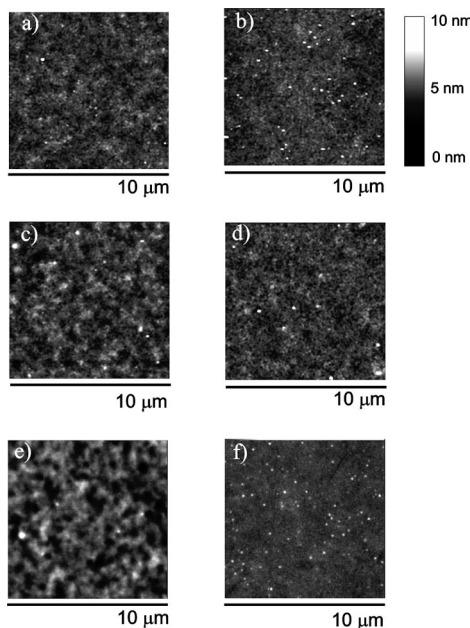


**Figure 3.** (a,c,e) Topography images by TM-AFM for layers grafted from 1.0 SAMs after 10, 15, and 20 min of photoirradiation, respectively. (b,d,f) Topography images by TM-AFM for layers grafted from 0.2 SAMs after 10, 15, and 20 min of photoirradiation, respectively.

observed are thus remarkably higher than the values for SIP of MMA initiated from a similar system.<sup>44,45</sup> However, the shapes of the thickening rate curves are rather similar to those that are typical of iniferter-mediated SIP.<sup>45</sup>

In addition, for all of the samples studied, an apparent induction time can be recognized as an initial slow thickening rate during the first 20–30 min of irradiation, followed by acceleration of the films' growth. Such a slow initial polymerization rate might be caused by radical transfer to oxygen that is still present in the reaction medium in the early stages of the process. More interestingly, as already observed by Metters et al., who studied the iniferter-mediated photografting of MMA, a slow initial increase in thickness followed by rapid growth can be interpreted to be a consequence of different configurations of the surface-tethered chains; namely, it is related to a mushroom-to-brush transition.<sup>45</sup>

It is also interesting that for all of the six different surface concentrations of initiator reported, no relevant slowing down of the film thickening was recorded after long irradiation times, and thus chain termination reactions do not seem to play a role in limiting the final thickness values that could be achieved.

Ellipsometry measurements of the film thickness showed no significant influence of the surface composition of the starting SAMs on the films' thickening rate. PMAA films grafted from

SAMs of DTCA (DTCA 1.0 in Figure 3a) with full coverage were shown to grow at a similar rate with respect to the cases in which DTCA molecules were diluted with DDS-inert analogues. This behavior was observed down to high dilutions, such as in the case of layers grafted from 0.2 SAMs (most diluted studied).

An explanation of this apparently unexpected behavior is offered by considering the effect of high surface concentration of radicals for high molar ratios of DTCA. In support of this idea, Baker et al.<sup>29</sup> observed that when ATRP was used the polymerization rate from SAMs with decreasing initiator concentrations did not show a relevant slowdown over a wide range of concentration. This result was justified by an increase in bimolecular termination reactions for high surface concentrations of the initiator and thus indirectly assumes that only a fraction of growing chains actually contributed to the formation of the grafted film when compared with the potential grafting points that are present in the precursor SAM. When the results obtained here are compared, this phenomenon seemed to play a more important role for iniferter-based initiators when compared with ATRP-based SIP.<sup>29</sup> If bimolecular termination strongly influenced the photografting of PMAA and considering that similar thickening rates were obtained even though the surface coverage of initiator was varied, then a high number of growing chains should have undergone deactivation in the early stages of SIP and, most importantly, in the case of high surface concentration of initiator. A similar conclusion was also derived by comparing the ellipsometric thicknesses of PMAA films obtained by varying the sample/lamp distance (light intensity and thus rate of radical generation) for the two extreme cases of the films grafted from 1.0 and 0.2 SAMs. (See Figure 1s in the Supporting Information). Also, in this experiment, no relevant differences were found between very concentrated and diluted initiating monolayers; therefore, in the case of 1.0 SAMs, the increment of generated radicals induced by a higher number of photons that reached the surface also seemed to be affected by recombination.

To monitor whether the occurrence of termination reactions influenced the micro/nanomorphology of photografted PMAA films, AFM topography images of PMAA films grafted from samples 1.0 and 0.2 were recorded in the early stages of polymerization, namely, after 10, 15, and 20 min (Figure 3a–f) of UV exposure.

As the AFM images show, for films grown from 1.0 SAMs, the average roughness (root mean square, rms) showed a significant increase following polymerization. We observed an increase in roughness from 0.9 nm (measured on an area of  $10 \times 10 \mu\text{m}^2$ ) after 10 min of photoirradiation to 1.0 nm after 15 min, reaching 2.0 nm following 20 min of reaction (corresponding to a 120% overall increase). However, in the case of PMAA layers grown from 0.2 SAMs (as can be seen by comparing Figure 3b,d,f), such strong roughening with polymerization time

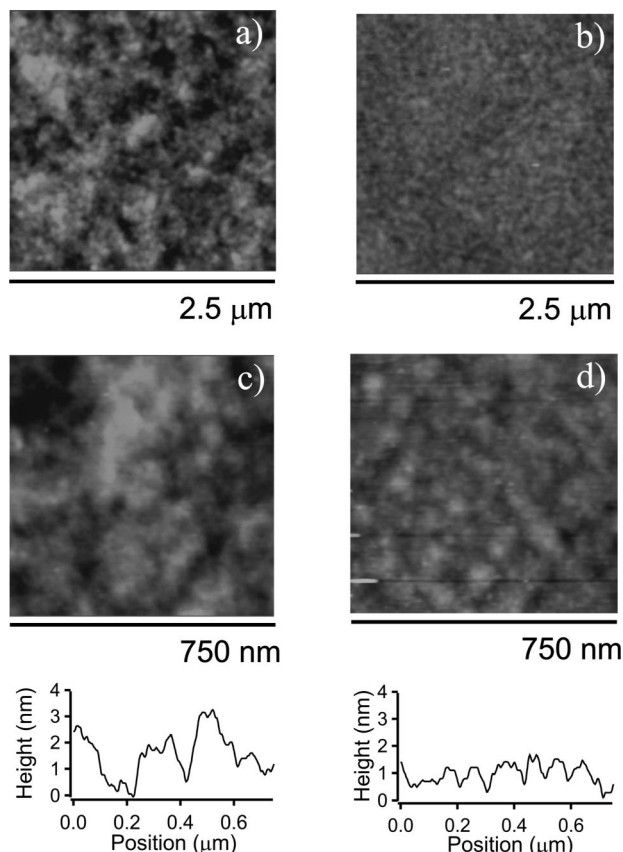


**Figure 4.** (a,c) High-resolution topography images by TM-AFM for layers grafted from 1.0 SAMs; the corresponding cross-sectional profile is given below. (b,d) High-resolution topography images by TM-AFM for layers grafted from 0.2 SAMs; the corresponding cross-sectional profile is given below (vertical scale from black to white: 10 nm).

was not pronounced. In the latter cases the average rms values after 10, 15, and 20 min of photografting were, respectively, 0.5, 0.6, and 0.7 nm (measured on an area of  $10 \times 10 \mu\text{m}^2$ ), with an overall increment of 40% during the polymerization time studied. (For the smoother films obtained from SAMs with low coverage, peculiar dotlike features of uniform size can be seen. We speculate that these might be precipitated chains grown in the solution.)

When the two different behaviors were compared, a higher roughening rate was found in the case of films grafted from SAMs with a high concentration of DTCA.

In addition to the average rms roughness, the surface nanomorphology also showed important differences in a comparison of films grafted from 1.0 and 0.2 SAMs. As can be seen in the high-resolution micrographs in Figure 4, in the case of 1.0 films, polymer aggregates with typical lateral dimensions ranging from 50 to 200 nm are present on the brush surface. These bunches of grafted macromolecules extend from the surrounding surface, producing peak-to-peak values that, in many cases, reach 2.5 to 3.5 nm (compare corresponding cross section). The surface of PMAA films grown from 0.2 SAMs showed a regular and continuous nanomorphology characterized by polymer structures presenting peak-to-peak values of 0.5 to 0.7 nm.

It has to be mentioned that an enhancement of surface roughness for grafted polymer films was related to cross-linking in some reports.<sup>47,48</sup> In the present case, we believe that surface asperities produced by polymer aggregates were caused by broader chains length distributions consequent to the high occurrence of termination reactions when PMAA films were grafted from 1.0 SAMs.

Aiming to confirm our theory, alternatively from 1.0 and 0.2 SAMs, we grafted PMMA, a polymer that is much more inert than PMAA toward possible spontaneous cross-linking, by following experimental conditions similar to those reported by Rahane et al.<sup>45</sup> Following 30 min of irradiation, the PMMA films were analyzed by TM-AFM. As can be seen by comparing the two images in Figure 2s in the Supporting Information, PMMA grafts grown from 1.0 SAMs presented enhanced surface roughness compared with films grafted from 0.2 SAMs and showed very similar morphological differences with respect to the correspondent PMAA films.

Differences in film thickness can be directly related to variation of molecular weight for grafted polymer chains in the brush regime;<sup>49</sup> therefore, marked peak-to-peak height values can also be interpreted as being caused by area constituted by chains of different length. Considering that this phenomenon was just found in the case of full SAMs of initiator molecules, it had to be related to very high concentrations of growing radicals. Therefore, a consequent increase in the occurrence of bimolecular termination, which influences the chain-length distribution of the grafted polymer, very likely also influenced the surface micro/nanomorphology of PMAA films grafted from 1.0 SAMs.<sup>50</sup>

PMAA films grown from 1.0 SAMs during short irradiation times are supposed to be formed by denser assemblies of grafts when compared with polymer films photopolymerized from 0.2 starting SAMs. Therefore, the two different layers, which present similar thicknesses ( $\sim 20$  nm by ellipsometry), should also show different resistance toward mechanical scratching.

An easy scratching experiment can thus highlight the completely different properties of the layers because polymer films that present comparable thicknesses but different densities of anchoring points to the underlying substrate should also show different mechanical resistance. An immediate demonstration of this peculiar behavior can be obtained by mechanically removing the dry films by using plastic tweezers and subsequently imaging the scratched regions with an optical microscope (Figure 5a,b). The PMAA film grafted from sample 1.0 could not be completely removed; however scratching removed virtually the entire contacted sections of the 0.2 films. These differences could clearly be seen after the scratching of the films when the two surfaces were wetted with a water drop. Comparing the insets of the two images in Figure 5a,b it can clearly be seen how the scratched regions of 0.2 could not be wetted, exposing the rather hydrophobic initiating SAMs, whereas the surface of 1.0 stayed completely covered by the water drop, evidencing much more resistance toward film detachment.

The swelling properties of these two different films should also be influenced if the mechanical and morphological differences were related to different chains characteristics. To investigate the swelling properties of PMAA, layers grafted from 1.0 and 0.2 SAMs were first scratched with plastic tweezers to accomplish the complete removal of polymer that was presented in the case of PMAA grafted from 1.0 SAMs. Following scratching, the samples were immersed in PBS solution (pH 7.0), and the height of the swollen grafts was measured by CM-AFM as the difference between scratched regions and the surrounding intact PMAA film (e.g., shown by the arrows in Figure 5a,b). Films presenting dry step heights of 20 and 30 nm (synthesized during 20 min of UV irradiation from 1.0 and 0.2 SAMs, respectively) when immersed in the liquid swelled profusely and reached heights of 500 and 550 nm when grown from 1.0 and 0.2 SAMs, respectively. The degree of swelling measured for the two layers was in good agreement with reported values for PMAA brushes synthesized by free radical polymerization methods;<sup>51</sup> nevertheless, no relevant differences

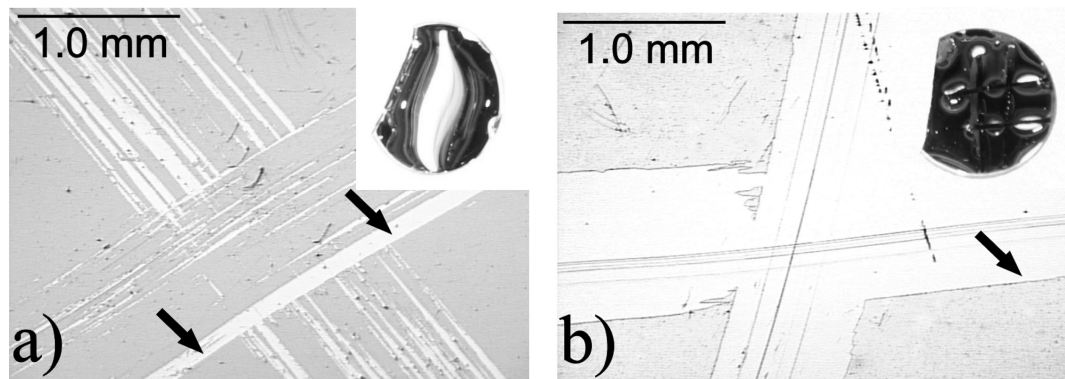


**Figure 5.** (a) Scratched films of PMAA grafted during 20 min of irradiation from 1.0 SAMs imaged with an optical microscope and (b) similar PMAA films grafted during the same polymerization time but from 0.2 SAMs. In the insets (size:  $3 \times 3$  cm<sup>2</sup>) of a and b, pictures from a digital video camera showing the wettability of the respective films over the scratched regions are shown. In regard to the arrows, see the explanation in the text.

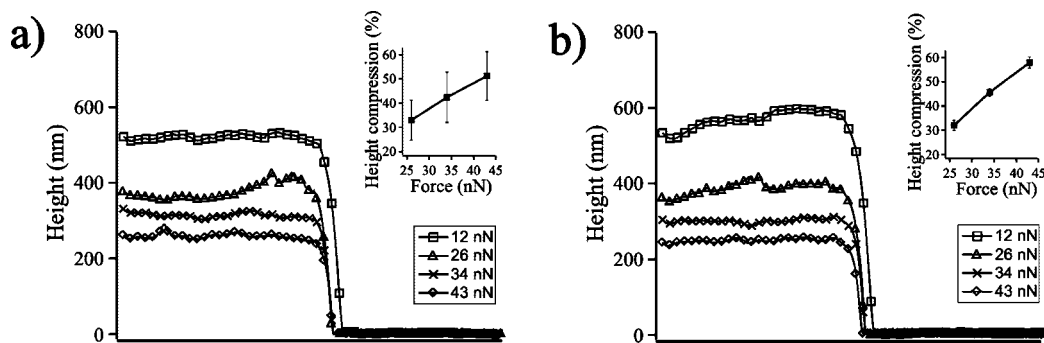


**Figure 6.** Representative cross sections showing the step height of PMAA films grafted from (a) 1.0 and (b) 0.2 SAMs recorded by CM-AFM in PBS solution at pH 7.4 by applying increasing load (from 12 to 43 nN). The corresponding insets in a and b show the compressibility values measured as the relative height decrease as a function of the load.

(within the experimental errors measured) were observed between the two samples, which would be expected in the case of different grafting densities.<sup>29,52</sup>

To test the compressibility of the two grafted layers in this medium, the edge of the polymer films was scanned, applying different loads by the AFM tip, and the step height between the polymer and the underlying substrate was recorded. In Figure 6a,b, typical cross sections depicting the height between the polymer films and the solid supports at different applied loads (at 12, 26, 34, and 43 nN) are shown, with the corresponding plots reporting the relative compressibility values normalized to the height observed at the lowest load (insets of Figure 6a,b, respectively, for films grafted from 1.0 and 0.2 SAMs). The average height of the film decreased under the increasing load in a similar way for both samples, but the films grafted from 1.0 showed a much higher variability in the compressibility, as evidenced by the much larger standard deviations in the inset of Figure 6a, when a large number of compression data from different sections of the film were compared. We believe that this larger heterogeneity is a result of the inhomogeneous morphology of this film.

In summary, distinct differences were observed from the morphological characterization performed in air and from the swelling properties of films synthesized after short irradiation times from very diluted and concentrated initiating SAMs, respectively. Because these films displayed similar growth rates in the entire range of polymerization time studied, it is possible to speculate that bimolecular termination reactions, which are predominant in films grown from 1.0, directly affected the film morphology and were presumably more frequent in the early stages of the polymerization process, that is, within the first 20 min of irradiation.

**In Situ Quartz Crystal Microbalance with Dissipation Monitoring Measurements.** To investigate the growth of PMAA in situ in the early stages of polymerization, we used Au-coated quartz crystals functionalized with 1.0 and 0.2 initiating SAMs as substrates for the subsequent photografting of PMAA. In the present study, the functionalized sensors were placed inside a QCM measurement cell equipped with a quartz window that could thus expose the substrate's surface to the external UV irradiation source in a cross-linking chamber. A degassed solution of MAA was pumped into the cell and fully covered the exposed functionalized sensor surface, and this setup was finally irradiated for 20 min, recording the  $\Delta f$  and  $\Delta D$  values as a function of the polymerization time.<sup>53</sup>

In Figure 7a,b is shown the frequency shift,  $\Delta f$ , recorded for three different overtones for polymerization performed on sensors modified with 1.0 and 0.2 SAMs, respectively. Following the frequency traces, the starting and the ending of the UV irradiation are highlighted by two arrows at times corresponding to 0 and 20 min, respectively. During this period, the decrease in resonant frequency, which was observed for both SAMs, corresponded to an increase in the mass coupled to the sensor, which was caused by the growth of surface-tethered polymer chains. The decrease in  $\Delta f$  was accompanied (Figure 7a,b) by a concomitant increase in dissipation,  $\Delta D$  (Figure 7c,d), which is consistent with the surface growth of hydrated polymer chains covering the sensor.

The onset of shifts in  $\Delta f$  and  $\Delta D$  was observed 5–7 min after the beginning of UV irradiation. Before that time, only a small transient increase in  $\Delta f$  due to the UV light itself on the sensor was observed. (See Figure 3s in the Supporting Information.) We interpreted this delay to be most likely due to an induction time during which the propagation of growing chains



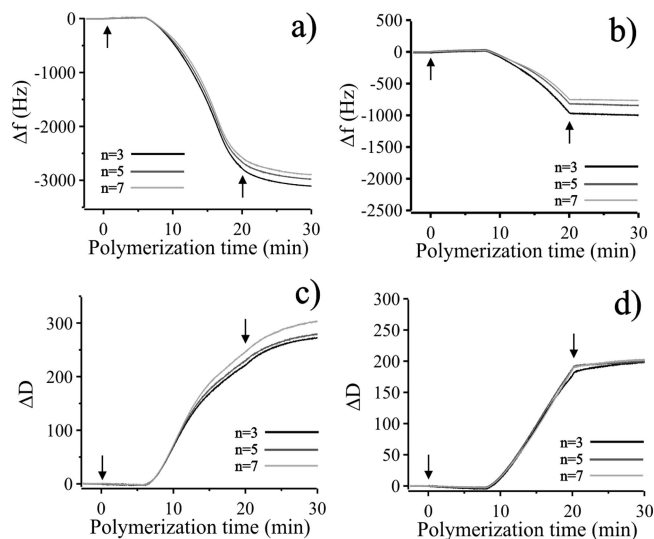


**Figure 7.** Change in (a,b) frequency  $\Delta f$  and (c,d) dissipation  $\Delta D$  of a QCM-D recording of the photopolymerization process. Starting and ending times are indicated by black arrows in the graphs. The changes in  $\Delta f$  and  $\Delta D$  were recorded, respectively, in the case of PMAA grafted from (a,c) 1.0 and (b,d) 0.2 SAMs.

is very slow and is also partially masked by the initial UV-induced transient response of the sensor itself.

Interestingly, the frequency decrease and dissipation increase for the two different SAMs did not follow the same kinetics and also had very different rates of change. The layers grown on 1.0 showed a faster  $\Delta f$  decrease and  $\Delta D$  increase compared with the photografting on 0.2 SAMs. Furthermore, after the UV light was switched off, for 0.2 initiating SAMs, the variations in  $\Delta f$  and  $\Delta D$  immediately leveled off, indicating the interruption of polymer grafting. In the case of 1.0 SAMs, instead, the variation rate of frequency and dissipation did not become 0 when UV was switched off. Instead it reached a steady state, slowly leveling off during 10 min following the end of the polymerization. We suggest that this phenomenon may be due to an increase in viscosity by polymerization initiated in the medium when films were grafted from 1.0 starting layers. In support of this assumption, we reason that the UV irradiation of MAA solutions, even in the absence of any initiating functionalized surface, were shown to induce a gradual decrease in  $\Delta f$  following the irradiation time. (See Figure 4s in the Supporting Information.)

The differences between the two samples become more evident if the mass uptake as a function of the irradiation time obtained by fitting the  $\Delta f$  and  $\Delta D$  response by using the Voigt model for the three overtones displayed was compared for 1.0 and 0.2 SAMs. The difference between the two trends in Figure 8 highlights the fact that the total film mass (expressed as ng/cm<sup>2</sup>) grafted from 1.0 SAMs exhibits a much more accelerated growth compared with that of the 0.2 SAMs during the first 20 min of polymerization. The measured values must be interpreted to be the total mass increment, considering the polymer chains to be hydrated and trapping a substantial amount of excess water and possibly monomers within the brush.

Whereas the increase in dry mass is relatively similar for the two initiator concentrations, once the growth has become significant (Figure 2), the increase in hydrated mass is much more rapid for the 1.0 SAMs and also starts earlier, as evidenced by the shorter lag phase observed. Furthermore, the ratio of  $\Delta D$  to  $\Delta f$  (roughly incremental viscous losses per mass unit adsorbed) that can be inferred from the data in Figure 8 (also, Figure 5s in the Supporting Information) is higher for the 0.2 SAMs than for the 1.0 SAMs, which indicates a denser, more

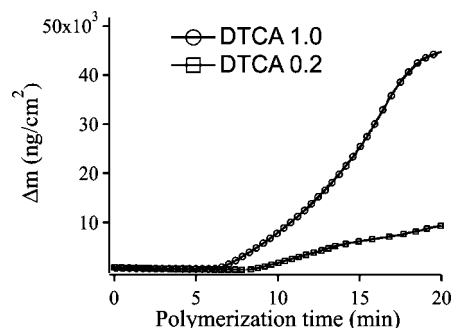


**Figure 8.** Hydrated mass uptake (expressed as ng/cm<sup>2</sup>) estimated by fitting  $\Delta f$  and  $\Delta D$  values obtained during the photopolymerization of PMAA to a Voigt model for the adsorbed film for 1.0 (○) and 0.2 (□) SAMs, respectively.

rigid film initially forming in the latter case, whereas it becomes similar after the slowdown in mass growth that occurs for the 1.0 SAM after 15 min.

These results demonstrate that a higher number of polymer chains were initially grafted from full initiator SAMs compared with initiating layers presenting DTCA diluted with DDS. In addition, most likely a consequence of the structural heterogeneity of 1.0 samples (evidenced by peculiar surface morphology and by film compressibility measures by AFM), the film can take up more water, as evidenced by the higher total hydrated mass. When dried, the amount of polymer for the two initiator coverages becomes comparable, as shown by ellipsometry. The very large difference between ellipsometric mass and QCM-D mass that was initially observed might also be partially related to a faster growing 1.0 SAM-initiated PMAA film because of the higher density of chains and because it was reproducibly observed that the Voigt modeled mass (as well as the untreated data) showed a significant decrease in growth rate between 15 and 20 min of irradiation and that the Voigt mass growth rates at 20 min became similar for high and low initiator density SAMs. Therefore, the crowding of growing chains favoring bimolecular reactions and affecting the subsequent thickening rate by decreasing the effective number of tethered macroradicals might become dominant around this time. As a consequence of this decrease in growing chains, the film thickening versus polymerization time showed very similar trends in the case of thick films grown from full layers of initiators with respect to SAMs where the initiators are diluted with inert adsorbates. The AFM images of dry films showing evidence of a higher structural heterogeneity for full iniferter coverage support this interpretation.

## Conclusions

We investigated here the photografting of PMAA using mixed initiating systems on the basis of SAMs containing iniferter-based adsorbates and demonstrated how the fine-tuning of the composition of the starting layers could influence the morphology and the properties of the subsequently grafted films.

Very thick PMAA grafts could be synthesized after relatively short reaction times for the entire range of surface concentration of the initiator studied. The film growth rate, measured with *ex situ* ellipsometry in the dry state, did not show a significant dependence on the composition of the starting SAMs, implying that radical recombination reactions played a role in the surface grafting process. By comparing the extreme cases of PMAA grafts from full SAMs of initiators and highly diluted SAMs, important morphological differences and different swelling properties were found after short irradiation times. We concluded that this is related to different kinetics of the grafting process in the two model substrates studied, as demonstrated by *in situ*

QCM-D measurements. Taking into consideration the initial film mass growth and viscoelastic properties for the two systems measured by QCM-D, a higher number of chains are initially grown in the case of concentrated SAMs of initiators. Nevertheless, because of termination reactions, this potential grafting efficiency did not turn into a higher thickening rate during the course of the polymerization with respect to films grown from diluted SAMs.

**Acknowledgment.** We thank Clemens Padberg for his precious technical support as well as the Commission of the European Union (Marie Curie RTN contract number MRTN-CT-2004-005516 BioPolySurf) and ETH Zurich for financial support.

**Supporting Information Available:** Ellipsometric thickness values for PMAA films grafted from SAMs, topography images by TM-AFM for PMMA layers grafted from SAMs, change in frequency  $\Delta f$  measured by QCM-D during the UV irradiation of the gold sensor immersed in milli-q water and 1M MAA, and change in  $\Delta D$  as a function of change in  $\Delta f$  for a QCM-D recording of the photopolymerization process. This material is available free of charge via the Internet at <http://pubs.acs.org>.

## References and Notes

- (1) Kaholek, M.; Lee, W. K.; Ahn, S. J.; Ma, H. W.; Caster, K. C.; LaMattina, B.; Zauscher, S. *Chem. Mater.* **2004**, *16*, 3688–3696.
- (2) Ahn, S. J.; Kaholek, M.; Lee, W. K.; LaMattina, B.; LaBean, T. H.; Zauscher, S. *Adv. Mater.* **2004**, *16*, 2141–2145.
- (3) Lee, W. K.; Caster, K. C.; Kim, J.; Zauscher, S. *Small* **2006**, *2*, 848–853.
- (4) Schrinner, M.; Polzer, F.; Mei, Y.; Lu, Y.; Haupt, B.; Ballauff, M.; Goldel, A.; Drechsler, M.; Preussner, J.; Glatzel, U. *Macromol. Chem. Phys.* **2007**, *208*, 1542–1547.
- (5) Boyes, S. G.; Akgun, B.; Brittain, W. J.; Foster, M. D. *Macromolecules* **2003**, *36*, 9539–9548.
- (6) Azzaroni, O.; Brown, A. A.; Cheng, N.; Wei, A.; Jonas, A. M.; Huck, W. T. S. *J. Mater. Chem.* **2007**, *17*, 3433–3439.
- (7) Magoshi, T.; Ziani-Cherif, H.; Ohya, S.; Nakayama, Y.; Matsuda, T. *Langmuir* **2002**, *18*, 4862–4872.
- (8) Matsuda, T.; Ohya, S. *Langmuir* **2005**, *21*, 9660–9665.
- (9) Mei, Y.; Wu, T.; Xu, C.; Langenbach, K. J.; Elliott, J. T.; Vogt, B. D.; Beers, K. L.; Amis, E. J.; Washburn, N. R. *Langmuir* **2005**, *21*, 12309–12314.
- (10) Harris, B. P.; Kutty, J. K.; Fritz, E. W.; Webb, C. K.; Burg, K. J. L.; Metters, A. T. *Langmuir* **2006**, *22*, 4467–4471.
- (11) Tugulu, S.; Silacci, P.; Stergiopoulos, N.; Klok, H. A. *Biomaterials* **2007**, *28*, 2536–2546.
- (12) Singh, N.; Cui, X. F.; Boland, T.; Husson, S. M. *Biomaterials* **2007**, *28*, 763–771.
- (13) Prucker, O.; Ruhe, J. *Langmuir* **1998**, *14*, 6893–6898.
- (14) Prucker, O.; Ruhe, J. *Macromolecules* **1998**, *31*, 602–613.
- (15) Matyjaszewski, K.; Xia, J. H. *Chem. Rev.* **2001**, *101*, 2921–2990.
- (16) Patten, T. E.; Matyjaszewski, K. *Adv. Mater.* **1998**, *10*, 901–915.
- (17) Shah, R. R.; Merceyes, D.; Husemann, M.; Rees, I.; Abbott, N. L.; Hawker, C. J.; Hedrick, J. L. *Macromolecules* **2000**, *33*, 597–605.
- (18) Chiefari, J.; Chong, Y. K.; Ercole, F.; Krstina, J.; Jeffery, J.; Le, T. P. T.; Mayadunne, R. T. A.; Meijs, G. F.; Moad, C. L.; Moad, G.; Rizzardo, E.; Thang, S. H. *Macromolecules* **1998**, *31*, 5559–5562.
- (19) Baum, M.; Brittain, W. J. *Macromolecules* **2002**, *35*, 610–615.
- (20) Georges, M. K.; Veregin, R. P. N.; Kazmaier, P. M.; Hamer, G. K. *Macromolecules* **1993**, *26*, 2987–2988.
- (21) Husseman, M.; Malmstrom, E. E.; McNamara, M.; Mate, M.; Mecerreyes, D.; Benoit, D. G.; Hedrick, J. L.; Mansky, P.; Huang, E.; Russell, T. P.; Hawker, C. J. *Macromolecules* **1999**, *32*, 1424–1431.
- (22) Bain, C. D.; Evall, J.; Whitesides, G. M. *J. Am. Chem. Soc.* **1989**, *111*, 7155–7164.
- (23) Bertilsson, L.; Liedberg, B. *Langmuir* **1993**, *9*, 141–149.
- (24) Folkers, J. P.; Laibinis, P. E.; Whitesides, G. M.; Deutch, J. J. *Phys. Chem.* **1994**, *98*, 563–571.
- (25) Atre, S. V.; Liedberg, B.; Allara, D. L. *Langmuir* **1995**, *11*, 3882–3893.
- (26) Jones, D. M.; Brown, A. A.; Huck, W. T. S. *Langmuir* **2002**, *18*, 1265–1269.
- (27) Wu, T.; Efimenko, K.; Vlcek, P.; Subr, V.; Genzer, J. *Macromolecules* **2003**, *36*, 2448–2453.
- (28) Harris, B. P.; Metters, A. T. *Macromolecules* **2006**, *39*, 2764–2772.
- (29) Bao, Z. Y.; Bruening, M. L.; Baker, G. L. *Macromolecules* **2006**, *39*, 5251–5258.
- (30) Tugulu, S.; Barbey, R.; Harms, M.; Fricke, M.; Volkmer, D.; Rossi, A.; Klok, H. A. *Macromolecules* **2007**, *40*, 168–177.
- (31) Huang, W. X.; Kim, J. B.; Bruening, M. L.; Baker, G. L. *Macromolecules* **2002**, *35*, 1175–1179.
- (32) Ma, H. W.; Hyun, J. H.; Stiller, P.; Chilkoti, A. *Adv. Mater.* **2004**, *16*, 338–341.
- (33) Benetti, E. M.; Zapotoczny, S.; Vancso, J. *Adv. Mater.* **2007**, *19*, 268–271.
- (34) Otsu, T.; Yoshida, M. *Makromol. Chem., Rapid Commun.* **1982**, *3*, 127–132.
- (35) Otsu, T. *J. Polym. Sci., Part A: Polym. Chem.* **2000**, *38*, 2121–2136.
- (36) *Polymer Handbook*, 4th ed.; Brandrup, J.; Immergut, H. E., Grulke, E. A., Eds.; Wiley: New York, 1999.
- (37) Rodahl, M.; Hook, F.; Krozer, A.; Brzezinski, P.; Kasemo, B. *Rev. Sci. Instrum.* **1995**, *66*, 3924–3930.
- (38) Sauerbrey, G. *Z. Phys.* **1959**, *155*, 206–222.
- (39) Hook, F.; Kasemo, B.; Nylander, T.; Fant, C.; Sott, K.; Elwing, H. *Anal. Chem.* **2001**, *73*, 5796–5804.
- (40) Reimhult, E.; Larsson, C.; Kasemo, B.; Hook, F. *Anal. Chem.* **2004**, *76*, 7211–7220.
- (41) Domack, A.; Prucker, O.; Ruhe, J.; Johannsmann, D. *Phys. Rev. E* **1997**, *56*, 680–689.
- (42) Voinova, M. V.; Rodahl, M.; Jonson, M.; Kasemo, B. *Phys. Scr.* **1999**, *59*, 391–396.
- (43) Cassie, A. B. D. *Discuss. Faraday Soc.* **1948**, *3*, 11–16.
- (44) de Boer, B.; Simon, H. K.; Werts, M. P. L.; van der Vegte, E. W.; Hadzioannou, G. *Macromolecules* **2000**, *33*, 349–356.
- (45) Rahane, S. B.; Kilbey, S. M.; Metters, A. T. *Macromolecules* **2005**, *38*, 8202–8210.
- (46) During this time interval, the viscosity of the reaction solution did not increase because no relevant amount of polymer in solution was formed by autoinitiation. For irradiation times of >80 min, solution polymerization was observed to take place and thus caused contamination of the polymer layers and affected the values of film thickness.
- (47) Edmondson, S.; Huck, W. T. S. *J. Mater. Chem.* **2004**, *14*, 730–734.
- (48) Pinto, J. C.; Whiting, G. L.; Khodabakhsh, S.; Torre, L.; Rodriguez, A. B.; Dalgliesh, R. M.; Higgins, A. M.; Andreasen, J. W.; Nielsen, M. M.; Geoghegan, M.; Huck, W. T. S.; Sirringhaus, H. *Adv. Funct. Mater.* **2008**, *18*, 36–43.
- (49) Halperin, A.; Tirrell, M.; Lodge, T. P. *Adv. Polym. Sci.* **1992**, *100*, 31–71.
- (50) Jordan, R.; Ulman, A.; Kang, J. F.; Rafailovich, M. H.; Sokolov, J. *J. Am. Chem. Soc.* **1999**, *121*, 1016–1022.
- (51) Biesalski, M.; Johannsmann, D.; Ruhe, J. *J. Chem. Phys.* **2002**, *117*, 4988–4994.
- (52) Cheng, N.; Azzaroni, O.; Moya, S.; Huck, W. T. S. *Macromol. Rapid Commun.* **2006**, *27*, 1632–1636.
- (53) The latter time of UV exposure was chosen to investigate the physical characteristics of the films during the initial polymer growth. The irradiation of MAA solutions for longer times would cause a large change in density and viscosity of the medium because of the formation of polymer in solution. This would greatly affect the response of the QCM-D and distort the interpretation of changes to the surface-polymerized film.

MA8014678